Conductivity and switching phenomena in Mn-doped perovskite single crystals and manganite thin films

N. Noginova, G. B. Loutts, and E. S. Gillman
Center for Materials Research, Norfolk State University, 700 Park Avenue, Norfolk, Virginia 23504

V. A. Atsarkin
Institute for Radio Engineering and Electronics, 11 Mokhovaya, Moscow, Russia

A. A. Verevkin
Yale University, New Haven, Connecticut 06520

(Received 23 October 2000; published 5 April 2001)

For better understanding of the charge-transport mechanisms in perovskite manganites, along with colossal magnetoresistance (CMR) materials, such as $La_{1-x}Sr_xMnO_3$, we study systems with decreased content of Mn ions, such as single crystals of $LaGa_{1-x}Mn_xO_3$ ($0<x<0.5$). The conductivity of all the systems in study can be described adequately with a nonadiabatic approximation of the hopping model with the values of the activation energy and resistivity coefficient strongly dependent on the concentration of Mn ions. Nonlinear voltage-current characteristics demonstrated switching to the low-resistivity state at high current density in $LaGa_{1-x}Mn_xO_3$ crystals as well as in CMR films of low crystallinity. We explain the obtained results based on the small-polaron-hopping model, taking into account the heating processes and percolation effects.

DOI: 10.1103/PhysRevB.63.174414 PACS number(s): 75.30.Vn, 72.20.−i, 72.80.Ga

INTRODUCTION

In the past few years, perovskite manganites (such as $La_{1-x}Sr_xMnO_3$, $La_{1-x}Ca_xMnO_3$, etc.) have attracted much scientific attention due to discovery of the colossal magnetoresistance (CMR) effect and rich complex diagram of phase transitions in these materials (see, for example, Refs. 1 and 2). Below a transition temperature, the materials demonstrate ferromagnetism and metalic behavior. At higher temperatures they are insulators with conductivity determined by a small polaron-hopping mechanism. According to the most theoretical models, magnetic and transport properties of these compounds are determined by magnetic interactions and electron exchange between Mn ions. Significant effects of electron-lattice interactions observed in CMR manganites[3] point to the important role of the lattice in transport and other properties of these materials. In spite of a great amount of experimental and theoretical studies devoted to CMR effect, many aspects of charge transport and electron-lattice interactions are still unclear.

On the other hand, high-resistivity perovskite materials with a very low concentration of Mn ions also exhibit interesting properties, related to charge transport and lattice distortion effects. As was recently found, the Mn-doped yttrium orthoaluminates, $Mn:YAlO_3$, demonstrate significant changes of absorption spectrum and refractive index under laser light illumination[4,5] and are of the great interest for holographic applications. A nonlocal photorefractive effect observed in $Mn:YAlO_3$ crystals is associated with distortions of the crystal lattice and processes of photoionization, electron transfer and trapping with participation of different Mn ion centers.[4] Finding of inter-relation between these phenomena and conductivity properties is of a great interest from both fundamental and applied points of view.

To better understand the mechanism of charge transport and related role of lattice effects in perovskites with different content of Mn ions, we have studied the intermediate case as well: materials with moderate concentration of Mn ions, single crystals of Mn-doped $LaGaO_3$ with concentration of Mn ions varying from 0.5% to 50%. In contrast to the well-known manganite CMR systems, in our single-crystal materials Mn ions are diluted by nonmagnetic Ga ions, which enter the same place in the crystal structure as Mn ions. Study of the conductivity and switching phenomena in these materials provides us with more detailed understanding of the transport mechanism in both the CMR materials and manganite perovskite materials without the coexistence of charge- and magnetic-ordering (Mn:LGO). As we show below, the switching phenomena in both these classes of manganite perovskites have the similar origin and are related to the percolation nature of the conductivity and existence of the macroscopic size clusters.

SAMPLES AND EXPERIMENTAL TECHNIQUES

Single crystals $LaGaO_3$, undoped and doped with 0.5%, 2%, 10%, 50% Mn, were grown by Czochralski technique. The undoped and 0.5% doped crystals have brownish color, the 2% crystal is dark-violet, the 10% and 50% doped crystals are black. In the crystals Mn ions could be expected to enter the Ga^{3+} sites and be in Mn^{3+} valence state. However, the spectroscopic studies[6] demonstrated also a presence of different valence states, such as Mn^{2+}, Mn^{4+}, and even small amount of Mn^{5+}. Likely, the other valences are produced by the excess of oxygen or the reaction of disproportionation in vicinity of the defects. According to Refs. 4, 7 and 8, the presence of different valence states of Mn is typical in perovskite materials even in the case of high-quality optically transparent crystals.

In the experiments with the thin epitaxial films we used

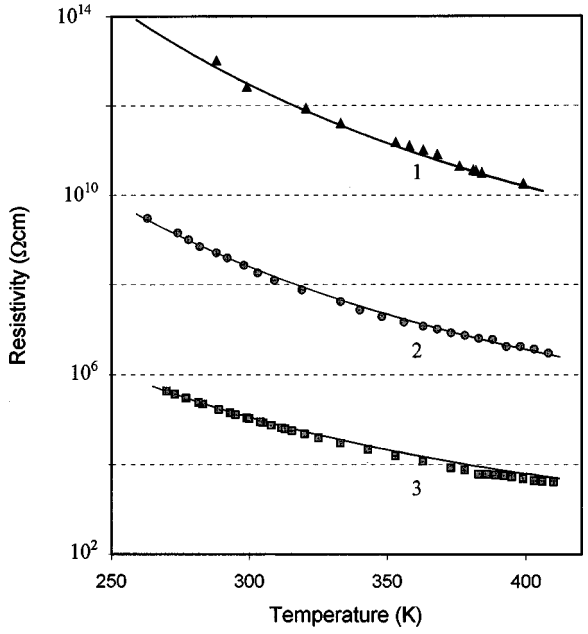

FIG. 1. Temperature dependence of the resistivity in $LaGaO_3$ crystals with 2% Mn ions doping concentration (1), 10% doping concentration (2), and 50% doping concentration (3). Solid curves are theoretical fits with $E_g = 583$ meV, $\rho_0 = 0.036\ \Omega$ cm/K$^{3/2}$ (2% of Mn ions), $E_g = 483$ meV, $\rho_0 = 0.0002\ \Omega$ cm/K$^{3/2}$ (10% of Mn ions), $E_g = 340$ meV, $\rho_0 = 2.45 \times 10^{-5}\ \Omega$ cm/K$^{3/2}$ (50% of Mn ions).

$La_{0.7}Sr_{0.3}MnO_3$ grown on $LaAlO_3$, MgO, and Al_2O_3 substrates, fabricated by metal-organic chemical vapor deposition (MOVCD) method. The thickness of the films was about 600 nm. A comparable study of the similar CMR films on Al_2O_3 and $LaAlO_3$ substrates[9] demonstrated that the films on Al_2O_3 substrates had much lower crystallinity and broader transition temperature range than high-quality films on $LaAlO_3$ substrates.

The conventional four-point contact technique was used in the conductivity measurements on the films, 50% and 10% Mn:$LaGaO_3$ samples. In conductivity measurements with low-doped Mn:$LaGaO_3$ crystals, we used single-crystal plates with the thickness of 0.2–0.4 mm with two electrical contacts mounted on the opposite sides.

EXPERIMENTAL RESULTS

A. Temperature dependence of low field conductivity

The voltage-current characteristics were linear at low enough currents. For currents higher than some critical value J_c, the resistance started to decrease. The value of J_c depended on the Mn-doping concentration. For 50% doped $LaGaO_3$, $J_c \approx 10^{-5}$ A ($j_c \approx 10^{-3}$ A/cm^2) for 10% and 2% doped samples J_c was less than 10^{-7} A ($j_c \approx 10^{-5}$ A/cm^2). For CMR thin films J_c was about 0.05–0.5 mA. Nonlinear behavior at higher currents will be discussed in next section.

To study temperature dependence of the resistivity $\rho(T)$, the current was chosen in the range $J \ll J_c$. Temperature dependences of the resistivity for Mn-doped $LaGaO_3$ crystals are shown in Fig. 1. The dependences are very similar to those observed in CMR films in paramagnetic phase,[1,2] where the mechanism of the conductivity is ascribed to the small-polaron hopping between Mn^{3+} and Mn^{4+} ions.

As known, in CMR materials, the concentration of Mn^{4+} ions practically corresponds to the concentration of divalent-charge compensators, (Sr, Ba, or Ca).[1,2] The excess of the oxygen in undoped $LaMnO_3$ materials also provides Mn^{4+} ions.[10] In accordance with this standard treatment let us suppose, that in the Mn:$LaGaO_3$ crystals as well, most Mn ions are in the valence state 3+. As was mentioned earlier, the crystals contain also Mn^{4+} and Mn^{5+} ions. Thus, we can expect that in our crystals, the conductivity should be associated with the similar hopping process from one Mn ion (Mn^{3+}) to another Mn ion (in valence of 4+ or 5+).

According to the small-polaron-hopping model,[11] the resistivity can be described by

$$\rho = \rho_0 T^{\alpha} \exp(E_g / k_B T), \tag{1}$$

where ρ_0 is the resistivity coefficient, T is the temperature, k_B is the Boltzmann constant, E_g is the activation energy, $\alpha = 1$ in the adiabatic case (when the hopping rate is much greater than the optical phonon frequency), and $\alpha = \frac{3}{2}$ in nonadiabatic case. As shown in Ref. 12, paramagnetic phase conductivity in CMR films can be described in the nonadiabatic approximation of the hopping theory. Obviously, the nonadiabatic approximation should be used for the materials with lower concentration of Mn centers, such as Mn:$LaGaO_3$ crystals, where the hopping rate is expected to be much slower due to greater distances between the Mn ions.

As one can see in Fig. 1, the resistivity in all the Mn:$LaGaO_3$ crystals can be well fitted with a hopping model in nonadiabatic approximation, supporting the fact that the mechanism of the conductivity is likely to be the same as that in CMR films: hopping of an electron between Mn centers. However, in our case, the concentration of Mn centers is not 100% as in CMR materials, but significantly lower corresponding to the Mn doping concentration in our crystals. The concentration of the carriers corresponds to the concentration of the Mn^{4+} (or $Mn^{4+} + Mn^{5+}$) in the frames of the standard models.

Figure 2 shows the activation energy as determined from Fig. 1 plotted as a dependence on the Mn ions concentration n. Our data on the activation energy in Mn:$LaGaO_3$ crystals (0.5–50 % doping concentration) are shown together with the data on the activation energy in Ga-doped $La_{0.67}Ca_{0.33}Mn_{1-x}Ga_xO_3$ materials, Ref. 13, where the concentration of Mn ions is high (90–100 %). The data on the inset are shown as a dependence on $n^{1/3} \propto 1/r$, where r can be considered as the mean distance between Mn ions. Note, that in spite of the slightly different composition (additional doping with Ca ions[13]), all the data follow the very similar dependence: a linear decrease of E_g with the decrease of $n^{1/3}$, varying from 80 meV in the crystals with 100% of Mn to about 640 meV in the crystals with 0.5% concentration of Mn ions. If we assume that the mechanism of the conductivity is the same in all the crystals, we could associate the increase of the activation energy with the increase of the hopping distance: the larger the hopping distance, the higher

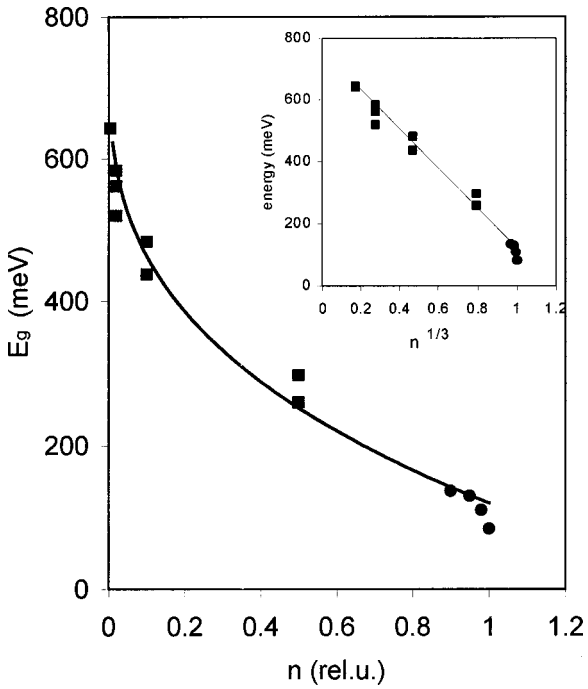

FIG. 2. Dependence of the activation energy on the concentration n of Mn in Mn:$LaGaO_3$ materials. Squares are our experimental data for Mn:$LaGaO_3$ crystals, circles are data for Ga doped $La_{0.67}Ca_{0.33}Mn_{1-x}Ga_xO_3$ (Ref. 13). Inset: dependence $E_g(n^{1/3})$. Curves are theoretical fits (see text below).

the activation energy. As one can see from Fig. 2, the dependence can be described as $E \propto (1/r_0 - 1/r)$, where r_0 is the constant.

Sensitivity of the hopping energy to particular composition was also reported in the CMR materials (see, for example Ref. 14, where the hopping energy changes from approximately 60 to 250 meV depending on the content of Mn^{3+} ions in $La_{1-x}Ca_xMnO_3$ thin films). As one can see from Fig. 2, in Mn:$LaGaO_3$, much stronger changes in activation energy are observed with decrease of the total Mn concentration.

The coefficient of resistivity ρ_0 also demonstrates strong dependence on the Mn concentration, increasing with the decrease in the Mn concentration, see Fig. 3. The inset shows the data on ρ_0 plotted as a function of the mean distance between the Mn centers r. One can see that all the experimental points can be fairly fitted by a straight line in the semilogarithmic scale, pointing to the nearly exponential dependence, $\rho_0 = A \exp(kr)$ with $k = 1.2 \times 10^8\ \mathrm{cm}^{-1}$ (see the dotted line in Fig. 3).

B. High electric field behavior

As has been previously mentioned, voltage-current curves for materials in this study can be considered as linear only at low enough currents. To study nonlinear effects at higher currents, we measured the voltage-current dependences for currents of 0.1–100 mA in the regimes of the constant current and the constant voltage. The measurements were performed slowly enough for the sample to reach an equilibrium

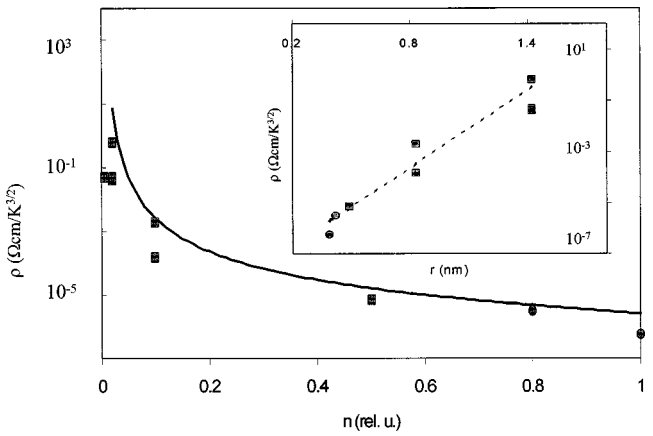

FIG. 3. Dependence of the resistivity coefficient ρ_0 on the concentration of Mn ions. Inset: ρ_0 as a function of the mean distance between Mn ions, r. Points, experimental data; dotted line, $\rho_0 \sim \exp(kr)$: solid line, fit with Eq. (2) (see discussion).

state, at ambient temperature $T = 300$ K. In the experiments with the constant voltage, starting from some critical value of electric field $F_d \sim 200$ V/mm for the 50% doped crystals, we observe rapid growth of the current with time, typical for an electric discharge. For the 10% doped sample, F_d was higher and approximately equal to 800 V/mm.

Results for the constant-current measurements are shown in Fig. 4. As one can see, in the 50% doped Mn:$LaGaO_3$ crystals [Fig. 4(a)], the voltage initially grows with the increase of the current and reaches maximum at some particular J_m. The further increase of the current leads to the decrease of the voltage (switching to the negative differential resistance, $R_d = dV/dI < 0$).

For the $La_{0.6}Sr_{0.4}MnO_3$ films, the situation is different, see Figs. 4(a) and 4(b). For the films of high crystallinity, grown on $LaAlO_3$ and MgO substrates, no switching has been observed. The increase of the current leads only to the saturation of the voltage-current dependence at high currents. However, the polycrystalline films on sapphire substrates demonstrates effects similar to those observed in Mn:$LaGaO_3$ crystals, see Fig. 4(b).

DISCUSSION

We start the discussion with the low-field (Ohmic) resistivity data taken at low-current measurements. The main ex-

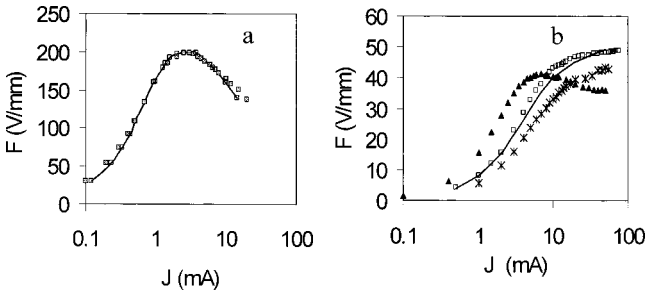

FIG. 4. Current-voltage dependences in 50% doped Mn:$LaGaO_3$ (a), and $LaSrMnO_3$ films (b) on substrates of Al_2O_3 (triangles), $LaAlO_3$ (squares), and MgO (stars). Solids lines are the fits with Eq. (9).

perimental findings are (i) the activation law, Eq. (1), for resistivity; (ii) a linear dependence of the activation energy E_g on quantity $n^{1/3}$, Fig. 2; and (iii) a nearly exponential dependence of the resistivity coefficient ρ_0 on r, Fig. 3. An explanation of these features can be based on the Holstein nonadiabatic theory of polaron mobility[11] further developed by Mott,[15] and Austin and Mott[16] as applied to the ionic lattice with the account made for the lattice distortions due to a trapped small polaron. Note the references mentioned above mostly consider the polaron hopping to the nearest-neighbor lattice site (at the distance a_0). In our case, mean distances r between the Mn centers in the Mn:$LaGaO_3$ crystals are longer (except for the 50% doped sample), and the hopping process must be more complicated and cannot be described accurately by the well-known theoretical expressions given in Refs. 11, 15 and 16. So we shall limit ourselves to a rather qualitative explanation of the observed temperature and concentration dependences and order-of-magnitude estimates.

The temperature dependence of the Ohmic resistivity (Fig. 1) was already discussed in Sec. 3 in terms of the nonadiabatic polaron hopping. To go further, a more detailed expression is needed. According to Refs. 11 and 16, at high enough temperatures ($T > \theta/2$, where θ is the Debye temperature) one has in the nonadiabatic limit

$$\rho = \frac{2\hbar E_g^{1/2}}{n_h e^2 l^2 \pi^{1/2} J^2} (k_B T)^{3/2} \exp(E_g / k_B T) \tag{2}$$

where $E_g = E_p/2$, E_p being the polaron binding energy; e is the electron charge; n_h is the concentration of carriers (in our case, the carriers are holes associated with Mn^{4+} or Mn^{5+} ions); l is the mean hopping distance; and

$$J = J_0 \exp(-r/r_p) \tag{3}$$

is the polaron band half-width determined by overlapping of the neighboring lattice polarization clouds.

Now we turn to the concentration dependence of the activation energy, Fig. 2. According to the small-polaron model,[15,16] the activation energy also depends on the lattice polarization clouds associated with a small polaron (such a role can be also played by the Jahn-Teller lattice distortions typical for the Mn^{3+} ions with d^4 electron configuration[17]). Namely, the following relation holds:[15]

$$E_g = (\tfrac{1}{4}) e^2 (1/\varepsilon - 1/\varepsilon_s)(1/r_p - 1/r), \tag{4}$$

where ε, ε_s are the high frequency and static dielectric constants, and r_p is the effective radius of the lattice distortion induced by a carrier. The best fit of the experimental data with Eq. (4) (shown with the solid line in Fig. 2) is obtained at $r_p = 0.32$ nm, in order-of-magnitude agreement with the nearest-interatomic distance.

Now let us discuss the concentration dependence of the resistivity coefficient ρ_0. Obviously, the observed nearly exponential dependence $\rho_0(r)$ (see Fig. 3) can be attributed to the factor J, see Eqs. (2) and (3), so that $k = 2/r_p$. However, Eq. (2) contains also other factors dependent on the Mn concentrations, such as $E_g^{1/2}$, l^2, and n_h^{-1}. $E_g(r)$ dependence is known from our experiments (see Fig. 2). Furthermore, l can be approximated by r. As to the carrier concentration, we cannot say anything definite at present; for a rough approximation, let us suppose n_h to be proportional to the total Mn concentration. Taking into account that for CMR materials $J \approx 6$ meV,[18] we calculated the corrected dependence, see solid curve in Fig. 3. This fit was obtained with values of $r_p = 0.2$ nm and the relative carrier concentration of 30%. From this fit, r_p is slightly less than that determined above from the E_g fit. In the content of these approximations, the agreement can be considered as a fairly good one.

Let us discuss the behavior of the materials at the high-current excitation. It is well known that such nonlinear effects and switching at high electric fields occur in materials with the high-negative temperature coefficient of conductivity such as some semiconducting glasses.[19,20] Using a similar approach, we assume that the temperature of the sample is

$$T = T_0(1 + bW) \tag{5}$$

where T_0 is the temperature of the sample holder, $W = j^*F$ is the heat power generated by the current, b is the coefficient dependent on the material and geometry of the conduction channel, and F is the electric field.

Substituting Eq. (5) into Eq. (1) obviously results in lowering the resistivity as the current increases and the heating appears. However, our experimental data could not be explained by taking into account the heating only. Let us take into consideration both the heating and the effect of the electric field on the hopping probability, which arises when the additional energy of a carrier due to the electric field F becomes comparable to $k_B T$. Assuming that the conductivity is determined by the hopping of the charge carriers between the wells of depth E_g, the current density depends on the electric field as[16]

$$j = 2 n_h e p d \exp(-E_g/kT) \sinh(edF/kT), \tag{6}$$

where d is the hopping distance and p is the hopping attempt frequency. From Eqs. (5) and (6), the current density is

$$j = 2 n_k e p d \exp\left(-\frac{E_g}{kT(1+bjF)}\right) \sinh\left(\frac{edF}{kT(1+bjF)}\right). \tag{7}$$

As shown in Fig. 4, our experimental data can be fitted well with the model above. The parameters b and d used for the fits are shown in Table I.

As one can see from Table I, the hopping distances evaluated from the theoretical fitting are much higher than the average distance between Mn centers. In our opinion, this can be explained by the percolation effect. As known, in the systems containing randomly distributed donor and acceptor centers, nonlinear effects in voltage-current dependence start much earlier as can be expected in homogeneous high-crystallinity materials.[21] In a percolation network, the voltage drops only at the resistors with the highest resistance that correspond to the donor-acceptor pairs separated by rather great distance $L \gg r$. In the assumption of the broad distribution of the activation energy, the cluster size L (the average

TABLE I. The average distance between Mn ions and parameters b and d used for fitting with Eq. (7).

Sample	$r=(1/n)^{1/3}$ (nm)	b (K/W mm)	d (nm)
10% doped Mn:$LaGaO_3$ crystal	0.9	0.4	220
50% doped Mn:$LaGaO_3$ crystal	0.52	0.3	160
$La_{0.6}Sr_{0.4}MnO_3/LaAlO_3$ film	0.385	0.29	1
$La_{0.6}Sr_{0.4}MnO_3/Al_2O_3$ film	0.385	0.6	8

distance between the resistors with highest resistance in the conduction network) can be estimated as[22]

$$L=\xi^{*}r, \tag{8}$$

where

$$\xi=1.74r/r_p+E_g/kT, \tag{9}$$

which yields $L\approx 7$ nm in 50% doped Mn:$LaGaO_3$, and $L\approx 18$ nm in 10% doped Mn:$LaGaO_3$, the numbers still lower than the values of d estimated in Table I. A possible reason for this discrepancy might be the fact that Eqs. (8) and (9) are worked out for the case of the so-called ''variable range hopping'' [21,22] that is not fully applicable in our experimental conditions. Note that the highest values of d are obtained for Mn:$LaGaO_3$ crystals, whereas for the single-crystal films this value is rather lower and in the order of the distance between Mn centers. Using conventional percolation arguments,[21,22] one can expect that the values for d listed in Table I are determined by the size of macroscopic clusters and characterize the clusters scale in our samples. The existence of such clusters can explain the switching effects observed in polycrystalline films and Mn:$LaGaO_3$ single crystals with broad distribution of Mn centers.

We should note that the switching phenomena at the extremely high current densities could be modified due to the lattice-phase transition. As known, at temperatures of 130 °C and higher, the crystals of $LaGaO_3$ exhibit the first-order phase transition.[23] As we found recently, the resistivity of Mn-doped $LaGaO_3$ crystals also demonstrated a transition from the high-resistivity state at lower temperatures to the low-resistivity state at higher temperatures. These results will be presented elsewhere.

CONCLUSION

We demonstrated that the conductivity in $LaGaO_3$ perovskites with the intermediate and low doping of Mn ions is determined by the nonadiabatic polaron-hopping mechanism, similar to that observed in CMR materials. The activation energy is strongly dependent on the dopant concentration, increasing with the reducing of the Mn concentration. The coefficient of resistivity ρ_0 has an exponential dependence as a function of r, that is also consistent with the polaron model.

The hopping conductivity could be expected to occur in photorefractive Mn:$YAlO_3$ (Refs. 4 and 5) crystals as well, where photoexcitation by laser light generates carriers due to photoionization of Mn^{4+} ions. Such mechanism of conductivity can allow carriers to travel for long distances hopping from one Mn^{4+} center to another. This is the most reasonable explanation for the high values of the effective diffusion lengths found earlier in two-beam-mixing experiments.[5]

The switching into low-resistance state at high enough currents was observed in the Mn:$LaGaO_3$ crystals and the CMR film of low crystallinity. This effect is likely related to the percolation nature of the conductivity in these materials and points to the existence of the macroscopic size clusters.

ACKNOWLEDGMENTS

This work was supported by NASA Grant No. NRA-99-OEOP-4 and DOE Grant No. DE-FG01-94EW11493. The authors would like to thank K.-H. Dahmen for providing the CMR thin films.

[1] A. P. Ramirez, J. Phys.: Condens. Matter **9**, 8171 (1997).
[2] J. M. D. Coey, M. Viret, and S. von Molnar, Adv. Phys. **48**, 167 (1999).
[3] A. Millis, P. V. Littlewood, and B. I. Shraiman, Phys. Rev. Lett. **74**, 5144 (1995).
[4] G. B. Loutts, M. Warren, L. Taylor, R. R. Rakhimov, H. R. Ries, G. Miller, M. A. Noginov, M. Curley, N. Noginova, N. Kukhtarev, H. J. Caulfield, and P. Venkateswarlu, Phys. Rev. B **57**, 3706 (1998).
[5] N. Noginova, W. Lindsay, M. A. Noginov, G. B. Loutts, and L. Mattix, J. Opt. Soc. Am. B **16**, 754 (1999).
[6] N. Noginova, M. A. Noginov, G. B. Loutts, and R. R. Rakhimov, in *Magnetoresistive Oxides and Related Materials*, edited by M. Rzchowski, M. Kawasaki, A. I. Millis, M. Rajeswari, and S. von Molnár, MRS Symposia Proceedings No. 602 (Materials Research Society, Pittsburgh, 2000).
[7] M. A. Noginov, G. B. Loutts, N. Noginova, S. Hurling, and S. Kuck, Phys. Rev. B **61**, 1884 (2000).
[8] J. W. Stevenson, M. M. Nasrallah, H. U. Anderson, and D. M. Sparlin, J. Solid State Chem. **102**, 175 (1993).
[9] J. J. Heremans, S. Watts, S. Wirth, X. Yu, E. S. Gillman, K. H. Dahmen, and S. von Molnar, J. Appl. Phys. **83**, 7055 (1998).
[10] I. Maurin, P. Barboux, Y. Lassailly, J.-P. Boilot, and F. Villain, J. Magn. Magn. Mater. **211**, 139 (2000).
[11] T. Holstein, Ann. Phys. **8**, 325 (1959).
[12] W. Westerburg, G. Jacob, F. Martin, and H. Andrian, J. Magn.

Magn. Mater. **196-197**, 536 (1999).
[13] Y. Sun, X. Xu, L. Zheng, and Y. Zhang, Phys. Rev. B **60**, 12 317 (1999).
[14] J. M. De Teresa, K. Dorr, K. H. Muller, L. Schultz, and R. I. Chakalova, Phys. Rev. B **58**, R5928 (1998).
[15] N. F. Mott, J. Non-Cryst. Solids **1**, 1 (1968).
[16] I. G. Austin and N. F. Mott, Adv. Phys. **18**, 41 (1969).
[17] Y. Tokura and Y. Tomioka, J. Magn. Magn. Mater. **200**, 1 (1999).
[18] M. T. Causa, M. Tovar, A. Caneiro, F. Prado, G. Ibanez, C. A. Ramos, A. Butera, and B. Alascio, Phys. Rev. B **58**, 3233 (1998).
[19] G. Feldman and K. Moorjani, J. Non-Cryst. Solids **2**, 82 (1970).
[20] S. R. Ovsinsky, Phys. Rev. Lett. **21**, 1450 (1968).
[21] B. I. Shklovskiy and A. L. Efros, Usp. Fiz. Nauk **117**, 401 (1975) [Sov. Phys. Usp. **18**, 845 (1975)].
[22] B. I. Shklovskiy, Fiz. Tekh. Poluprovodn. **10**, 1440 (1976) [Sov. Phys. Semicond. **10**, 855 (1976)].
[23] M. Berkowski, J. Fink-Finowicki, W. Piekarczyk, L. Perchu, P. Byszewski, L. O. Vasylechko, D. I. Savytskij, K. Mazur, J. Sass, E. Kowalska, and J. Kapuniak, J. Cryst. Growth **209**, 75 (2000).